CRIMSON PUBLISHERS
Wings to the Research

Archaeology & Anthropology: Open Access

ISSN: 2577-1949

Research Article

Detrital Zircon U-Pb Age and Petrographic Composition from Foreland Sediments of the Tansen Basin, Central Nepal: Constraints on Sediment Provenance and Tectonics of the Central Himalaya

Bhupati Neupane[1,2]* and Junmeng Zhao[1,2]

[1]*Key Laboratory of Continental Collision and Plateau Uplift, Institute of Tibetan Plateau Research and Centre for Excellence in Tibetan Plateau Earth Sciences, China*

[2]*University of Chinese Academy of Sciences*

***Corresponding author:** Bhupati Neupane, Key Laboratory of Continental Collision and Plateau Uplift, Institute of Tibetan Plateau Research, and Centre for Excellence in Tibetan Plateau Earth Sciences, Chinese Academy of Sciences, Beijing 100101, China

Submission: July 02, 2017; **Published:** October 04, 2018

Abstract

Foreland basin deposits of the Tansen Group of Lesser Himalayan association in central Nepal record passive margin sedimentation of the Indian continent with direct deposition onto eroded Precambrian rocks, succeeded by detritus from orogenesis as the Indian continent collided with Asia on a north-dipping subduction zone. Samples collected from Tansen Basin (Amile, Bhainskati, and Dumri formations), Higher and Tethys Himalaya were examined detrital zircon U-Pb dating and through petrographically. The Cretaceous-Paleocene Amile Formation is dominated by a broad detrital zircon U-Pb~1830Ma age peak with hosts a significant proportion (23%) of syndepositional Cretaceous zircons (121 to 105Ma) would be contributions from the Lower Lesser Himalayan volcanosedimentary arc, Gangdese batholith (including Xigazeforearc). The Bhainskati and Dumri Formation of the Tansen Group are more similar to Tethyan units than to Higher Himalaya Crystalline (HHC). The presence of ~23+/-1Ma zircons from the Higher Himalaya unit suggests that they could not have been exposed until the earliest Miocene time. Petrographic results indicate their "Quartzose recycled" and "recycled orogenic" suggesting Indian cratonic and Lower Lesser Himalayan (LLH) sediments as the likely source of sediments for the Amile Formation, the Tethyan Himalaya (TH) and Upper Lesser Himalaya (ULH) as the source for the Bhainskati Formation, and both the Tethyanand Higher Himalaya as the major sources for the Dumri Formation.

Keywords: Foreland basin; U-Pb Zircon ages; Petrographic results; Provenance analysis

Introduction

The Himalayan foredeep basin formed on the Paleozoic through early Cenozoic Tethyan continental margin of the Indian Plate [1,2]. The Cretaceous-Paleocene sedimentary basin (Tansen Basin), located in the southern part of the Lesser Himalaya, deposited on an eroded surface of Precambrian basement of the Lesser Himalaya [3,4]. The foreland basin sequences of the Nepal Himalaya are mostly continental deposits (some marine beds) developed first in a passive-margin setting [1] succeeded by detritus from the collision of the Indian plate with the Asian plate about ca.60-50Ma [5]. Although some recent studies have suggested that the initial India-Asia collision took place at ~34Ma [6-9], whereas Najman et al. [10] suggests the terminal collision of India with Asia took place at 54Ma.

The continuing tectonic following the upliftment process of the mountain ranges of the Lesser Himalaya (LH), the Higher Himalaya (HH), and Tethys Himalaya (TH) took place and ultimately were weathered and eroded and the foreland basin was over filled by their detritus [4]. In the sediments of the Tansen Basin, with the changing tectonics from passive-margin setting to a basin adjacent continental collision one can examine the changes in the sediment composition and style [11]. Sandstone composition can contribute information for reconstruction of the paleogeography, paleotectonic, and paleoclimate [12,13].The previous research pointed to an intimate relationship between detrital sand composition (bedrock composition of the sources) and tectonic setting [14-17]. Weltje [17] emphasised the significance of using statistically rigorous confidence intervals in ternary diagrams. Relatively few studies had been done mainly focusing on the U-Pb dating based on detrital zircon [1,18,19] rather than the petrographic study. The purpose of this study is to document the stratigraphy, U-Pb zircon age and petrography from a complete foreland basin section (Eocene and younger Tansen Basin) in central Nepal and to examine potential source rocks (HH and TH, one field traverse) for detrital infill.

Geological Setting and Stratigraphy

The Nepal Himalaya (800-km-long) occupies the central sector of the east-west trending 2,400km-long Himalayan range [20] and is divided into four tectonostratigraphic zones from south to north; the Tethys Himalaya, Higher Himalaya, Lesser Himalaya and Sub-

Himalaya (Siwaliks) (Figure 1) [21]. These tectonostratigraphic zones are bounded and separated by several south propagating, north dipping thrust/fault systems in different time spans. The South Tibetan Detachment System (STDS) separates the high grade crystalline metamorphic rock containing Higher Himalaya to the number of fold and fossils horizon of Eocene sedimentary units of Tethys Himalaya towards the north [22] while the Main Central Thrust (MCT) separates the crystalline belt of HH [23]. The Main Boundary Thrust (MBT) separates LH [24,25] from the Siwaliks where the Main Frontal Thrust (MFT), separates the Miocene-Pliocene Siwalik Zone [26] from the quaternary deposit; Indo-Gangetic Plains (Figure 1).

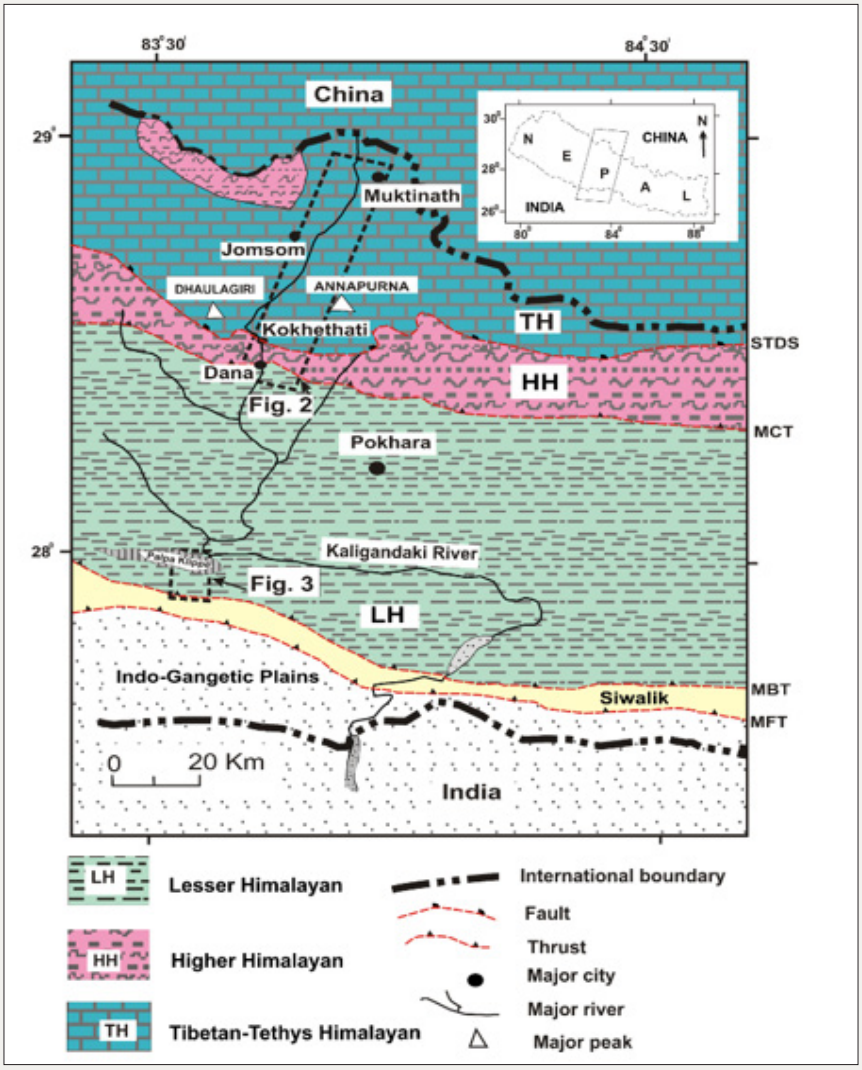

Figure 1: Simplified geological map of Nepal Himalaya in the region of the Kaligandaki River modified after Upreti & Le Fort [21]. Locations of Figure 2 & 3 are indicated by rectangular broken lines.
STDS: South Tibetan Detachment System; MCT: Main Central Thrust; MBT: Main Boundary Thrust; MFT: Main Frontal Thrust

Based on conventional geologic evidence and isotopic data, the LH rock units classified into Upper and Lower units in Nepal [1,25,27], which is supported by a similar classification of LH in India [24] and Bhutan. Lower Lesser Himalaya (LLH) contains the Paleo- to Mesoproterozoic rocks unconformably overlain by upper Paleozoic to Cenozoic rocks and Upper Lesser Himalaya (ULH) comprises Neoproterozoic metamorphic rock [25]. LH is correlated with the peninsular Indian Vindhyan Supergroup and other series of rocks [28]. The Vindhyan Super group; an intracratonic basin, is the thickest Precambrian sedimentary succession of west-central India and the duration of its deposition is one of the longest in the world [29].

Tethys himalaya (TH)

~40km long Tethys Himalaya, overlies along the STDS and extends north into Tibet (Figure 2); [30]. It lies between the STDS, a north-dipping normal fault in south, and the Indus-Tsangpo Suture Zone (ITS) in north. In Nepal, the TH fossiliferous sedimentary successions including shale, sandstone and limestone are well exposed in ThakKhola (Mustang), Manang and Dolpa areas [30]. A low-grade metamorphism can be observed adjacent to the thrust contact with the HH. The rocks are Paleozoic to Cenozoic in age and make up the hanging wall of the STDS (Figure 2); [31] were deposited on the northern passive margin of the Indian continent [22]. On the basis of lithostratigraphic section, from bottom to

How to cite this article: Bhupati Neupane. Detrital Zircon U-Pb Age and Petrographic Composition from Foreland Sediments of the Tansen Basin, Central Nepal: Constraints on Sediment Provenance and Tectonics of the Central Himalaya. Arch & Anthropol Open Acc .3(2). AAOA.000558. 2018.
DOI: 10.31031/AAOA.2018.03.000558

top the TH is divided into nine formations; Annapurna Yellow Formation, Sombre Formation, Tilicho Pass Formation, Tilicho Lake Formation, Jomsom Formation, Lumachelle Formation, Spiti Formation, Chuck Formation and Muding Formation (Figure 2).

Higher himalaya (HH)

Higher Himalaya (HH) is the Central Crystalline Zone made up of the Precambrian rock units, dominantly high-grade metamorphic rock and granitic gneiss [32]. It comprises mainly kyanite-sillimanite-bearing gneiss, schist, marble, and granite. It lies to the north of the Main Central Thrust (MCT) and is separated from the TH by the STDS (Figure 2); [25]. This crystalline unit extends continuously along the entire length of the mountain belt [23] and is commonly called the Higher Himalayan Crystalline Series (HHCS). Bordet et al. [33] sub-divided the HHCS into four units as kyanite-sillimanite gneiss, pyroxenicgneiss, and marble, banded gneiss and augen gneisses in order of higher structural position. However, Le Fort [20] divided into three Formations namely: Formation I, II, and III (Figure 2). There are sparse Miocene-aged igneous rocks (i.e., leucogranites) intruding HH as well as TH [34].

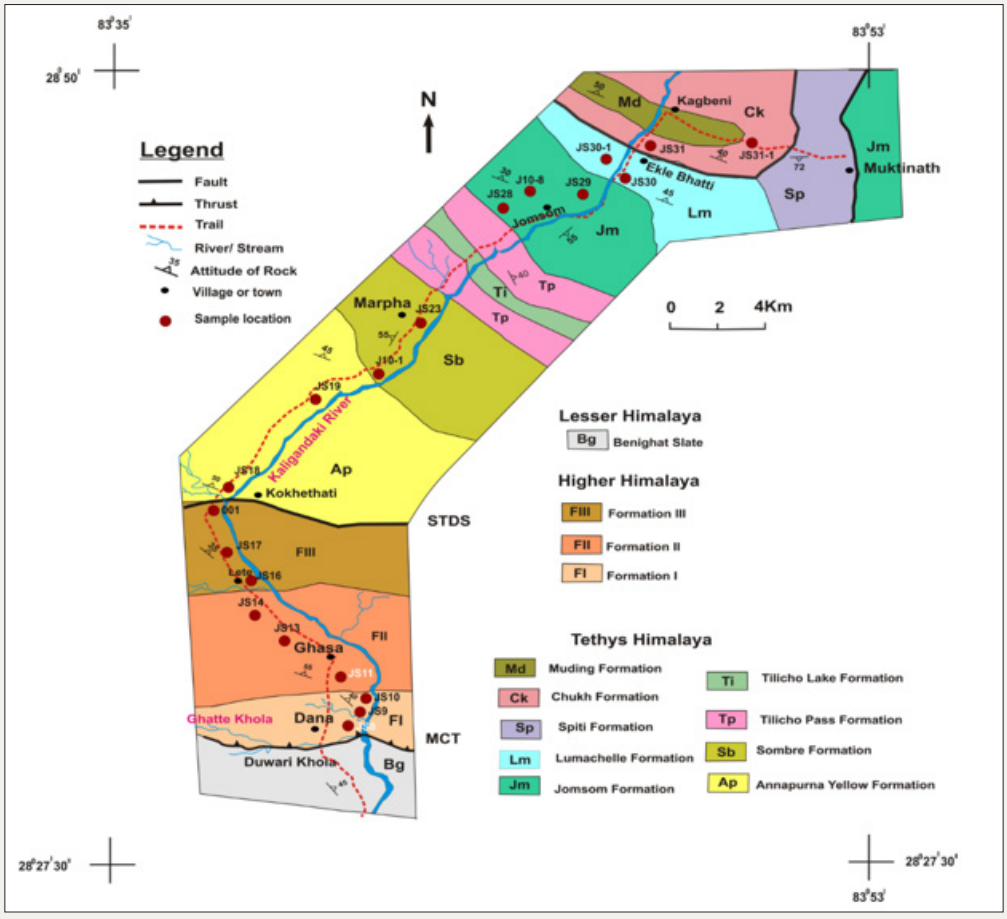

Figure 2: Generalized geological Map of Higher Himalaya and Tethys Himalaya [30].
MCT: Main Central Thrust; STDS: South Tibetan Detachment System
Samples locations are indicated by a red circle.

Tansen basin

Tansen foreland Basin succession, occurred in the upper LH, is about 2,400m thick succession deposited in non-marine environments, with some periodic marine incursions and finally the fluvial environment [3]. The unit was folded into a syncline in the Himalayan orogeny and currently the syncline is underlain and overlain by the portions of Precambrian Kaligandaki Supergroup (Figure 3). The abundant fossils and lithological succession in the Tansen area have been well studied by Sakai [3] and further classified into five formations (Figure 3): Sisne Formation, Taltung Formation, Amile Formation, Bhainskati Formation and Dumri Formation.

Sisne Formation is the lowest unit of the Tansen Group overlain on the Precambrian basement rocks of the Indian Plate (Kerabari Dolomite) of the Kaligandaki Supergroup and is disconformably overlain by the Taltung Formation (Figure 3). The Taltung Formation is further divided into lower and the upper member. The lower member comprises thick conglomerate (Charchare Conglomerate) at the type locality area and the upper member is characterized by carbonaceous shale containing the fossil plant

How to cite this article: Bhupati Neupane. Detrital Zircon U-Pb Age and Petrographic Composition from Foreland Sediments of the Tansen Basin, Central Nepal: Constraints on Sediment Provenance and Tectonics of the Central Himalaya. Arch & Anthropol Open Acc .3(2). AAOA.000558. 2018.
DOI: 10.31031/AAOA.2018.03.000558

genera Ptillophyllum, Cladophrebis, Elatocladus and Pterophyllum, indicating the age of the formation as Jurassic-Lower Cretaceous [3]. Similarly, the lower member comprising fining-upward cyclic sequence and upper rhythmic sequence member suggest that the formation was deposited in a gravelly braided and meandering river system.

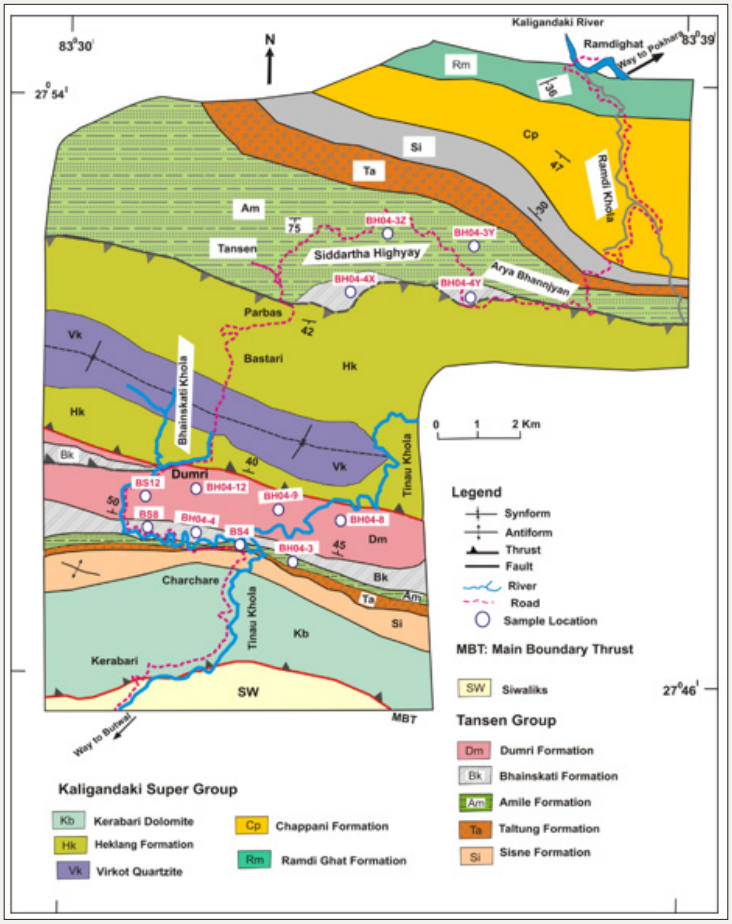

Figure 3: Generalized geological Map of Tansen Basin [3]. Sample locations are indicated by a white circle.

Amile formation (Am)

A ~35cm thick Amile Formation comprises hematitic conglomerate at the basal part and quartzose as well as carbonaceous sandstone, with coalified wood fragments and sporadic limestone beds at the upper part. Several marine fossils (e.g. bivalves, gastropods, echinoids, and corals) are abundant in limestone beds indicating the age of the formation as Cretaceous-Paleocene [3]. There is an unconformable contact between Am and the underlying Ta. The white quartzite beds are very coarse-grained, poorly sorted, silty sandstone or silt with red-purple siderite and rhodochrosite specks [35].

Bhainskati formation (Bk)

Black shale with thin alternations of calcareous and fossiliferous horizons Bhainskati Formation in central Nepal is considered to be Middle to Late Eocene on the basis of abundant foraminifera and other marine fossils. It consisting of green-reddish-purple pencil cleavage shale and some dark shale containing pyritized wood fragments, together with dark and muddy limestone and hematite beds, conformably overlies the Am. A fossiliferous horizon, coquina, is present in this formation. The lower part of the Bk contains abundant marine fossils like bivalves, gastropods, and particularly the presence of foraminifera Nummulitessp. indicates the age of this formation as Eocene [3]. However, middle pert includes brackish water molluscs, including Polymesoda and Bitissa, and skeletal fragments of land mammals and Trinychoidea [3].

Dumri formation (Dm)

The Dumri Formation is the first fluvial deposit in the Himalayan foreland basin [3] occupies as uppermost sequence of the Tansen Basin; and existed conformably above the Bk (Figure 3). It composed dominantly of medium-grained, bluish-gray to greenish-gray sandstone interbedded with red purple and green shale. This formation consists of arhythmicsequence of sandstone and shale, coalified trees all indicating rapidly deposited flood-plain depositional environment [3]. The proportion of shale decreases upward in the section, and intra-formational shale-pebble conglomerates and conglomeratic sandstones are more common in the upper parts of the formation. The biostratigraphy study constrains the age of the Dmation as early- to mid-Miocene [3] and considered as pre-Siwalik sediments [36].

How to cite this article: Bhupati Neupane. Detrital Zircon U-Pb Age and Petrographic Composition from Foreland Sediments of the Tansen Basin, Central Nepal: Constraints on Sediment Provenance and Tectonics of the Central Himalaya. Arch & Anthropol Open Acc .3(2). AAOA.000558. 2018.
DOI: 10.31031/AAOA.2018.03.000558

Research Methods

For the U-Pb detrital zircon analysis we selected 9 samples from the Himalayan transect (i.e. 3 from each unit; TH, HH and Tansen section). Zircon grains were separated by heavy mineral separation techniques. More than 250 detrital zircon grains from each sample were mounted in epoxy and polished close to one-third of the individual grain diameter. Detrital zircon U-Pb geochronology was conducted by laser-ablation inductively coupled-plasma-mass spectro-metry (LA-ICP-MS), attached with ESI New Wave laser (193nm ArF excimer laser) system with a Trueline (2 volume) ablation cell, at the Queensland University of Technology (QUT), Australia. Regarding the age probability plots, an Excel macro program was used that normalized individual curves based on the number of consistent analyses. Each curve includes the same area and then stacks the probability curves [1]. Temora2 was used as the primary standard and Plesovice as a monitor standard [37]. We present the detrital zircon ages that are concordant (of equal age) within uncertainties. In the present study, we dated a maximum of 100 grains from each sample. Those detrital U-Pb zircon dates within 10% discordance were accepted to construct the detrital zircon age spectra. Consequently, grains that were discordant at this stage were corrected for common Pb and Pb loss using the Andersen correction method in Iolite [38,39]. We report ages that are older than 900Ma, 207Pb/206Pb ages are quoted, while those younger than 900Ma represent 206Pb/238U ages [40]. Common Pb-corrected ages are used for ages <950Ma if the 208-based correction makes the analysis concordant, or in the case of an already concordant grain if correction improves concordance [1]. The vast majority of data that is discordant have had Pb loss. Petrographic thin sections (9 for HH and 11 for TH) were prepared and more than 300 grains per sample were counted under polarized light microscope (ZEISS Axio Scope. A1), following the GD point-counting method [41,42] in the Key Lab of Computational Geodynamics of Chinese Academy of Sciences, College of Earth Sciences, University of Chinese Academy of Sciences, Beijing.

Results and Analysis

Detrital zircon U-Pb ages.

Tethys himalaya (TH)

Three representative samples (JS18, JS10-1, and JS10-8) of TH were selected for the U-Pb detrital zircon analysis. Sample JS18 was taken from the lower part of Annapurna Yellow Formation, near the STDS. Out of 86 zircon ablations, we obtained 82 concordant ages. Three broad age clusters from this sample are 400 to 1100, 1400 to 1950 and 2300 to 2600Ma. The youngest group is strongly skewed toward the young end with dominant probability plot peaks at 510 and 600Ma (Figure 4A). Sample JS10-1 was taken from the lower part of Sombre Formation (Figure 2). From the total of 111 concordant grains of 133 ablated, 79 (71%) are less than 1200Ma and all are greater than 470Ma. A total 17 dated grains are between 502-568Ma forming a probability peak at 530Ma and there is another major peak at 870Ma and a minor one at 660Ma. For the 32 Precambrian grains, there are age clusters about 1400Ma, 2600Ma and two near 3300Ma. Sample JS10-8 is from Jomsom Formation (Figure 2), a fine-grained, thin- to medium-bedded gray-colored sandstone bed. From the 72 (of 110 ablated) the probability plot indicates 4 major age groupings: 400-600, 650-950 and 1000-1400 with a cluster between 1650 and 1920, and 4 Archean grains. Twenty grains (28%) are less than 610Ma. The probability peaks are at 500, 875 and 1140Ma. The minimum and maximum detrital zircon ages of this sample are 395Ma and 3271Ma.

Higher himalaya (HH)

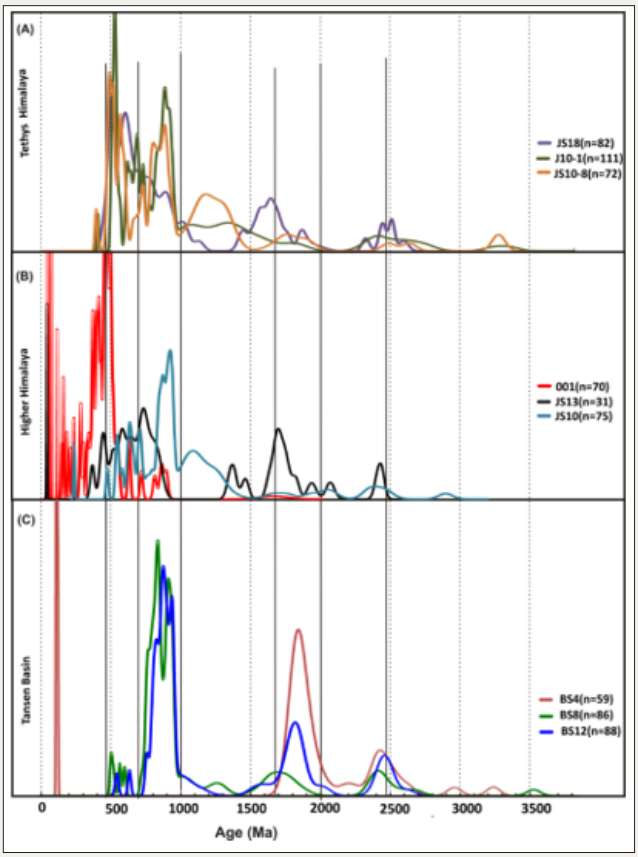

Figure 4: U-Pb relative age probability diagrams for the three groups of rocks analyzed in this study.
Figure 4A: TH: Purple= Ap, Green= Sb, Orange= Jm.
Figure 4B: HH: Blue= FI, Yellow= FII, Red= FIII.
Figure 4C: Tansen Basin: Red=Am, Green=Bk, Blue=Dm. The vertical black bars allow alignment of age data from Tansen samples to their possible sources. From oldest to youngest the lines delineate the top of the 2400Ma peak, surround the limits of the 2000 to 1600Ma peak (~1830Ma), surround the 950-750Ma peak and mark the youngest grain in the Tansen ignoring the Cretaceous zircons.

Three representative samples (JS10, JS13 and 001) from HH section (i.e., Formation I, II and III, respectively; Figure 2) were taken for the U-Pb detrital zircon analysis. For the granitic gneiss sample JS10 (FI), 100 detrital zircon grains were analyzed among them 75 are concordant. Most ages fall between 400 and 1350Ma with a dominant probability plot peak at 915Ma and lesser peaks at 530, 623, 693, and 1080Ma subordinate cluster at 2350Ma. There is one standout relatively young age at 220Ma. A single gneiss sample (JS13) was analyzed from Formation II. Altogether, 107 detrital zircon grains were systematically dated but only 37 were concordant because most grains have suffered significant Pb loss.

How to cite this article: Bhupati Neupane. Detrital Zircon U-Pb Age and Petrographic Composition from Foreland Sediments of the Tansen Basin, Central Nepal: Constraints on Sediment Provenance and Tectonics of the Central Himalaya. Arch & Anthropol Open Acc .3(2). AAOA.000558. 2018.
DOI: 10.31031/AAOA.2018.03.000558

Most grains are 580 to 1250Ma but the discordant grains suggest Archean populations as well. There are 3 Paleozoic ages (400 to 380Ma), one Cretaceous age (96Ma) and two Tertiary ages of 48 and 34Ma although, the zircon ages of Cretaceous -Tertiary are metamorphic and therefore would not form part of the detrital zircon age spectra. Himalayan metamorphism causing small degree partial melts with Pb loss in ancient zircons is a likely explanation for the ages observed in this gneiss. In the upper section of Formation III, sample 001 (Figure 2) was selected for U-Pb analysis. A total 113 detrital zircon grains were ablated and 70 concordant grains have been plotted (Figure 4B). Most grains are 550 to 260Ma, with 10 grains <250Ma ranging including Triassic, Jurassic, Cretaceous and Paleogene ones, the youngest being ~26Ma.

Tansen basin

The selected 3 samples for the U-Pb detrital zircon analysis, zircon grains were sub-rounded to sub-angularin shape and show oscillatory zoning. Sample BS 4, taken from the middle part of Am, is a fine-grained, medium- to thick-bedded gray-colored sandstone bed. From a total of 59 robust ages from 95 ablations, 75% grains are older than 1780Ma with the oldest age at 3240Ma and a clustered peak age at 1830Ma. This sample contains Paleoproterozoic zircons, and a few grains contain 14 Cretaceous zircons (25% of the sampled population) with ages between 105 and 121Ma (Figure 4C). The Cretaceous zircons are roughly syndepositional given the suspected formation age from fossil evidence. Altogether, 96 detrital zircon grains were analyzed for the sample (BS 8) in the Bk and 86 yielded concordant ages. The youngest age was 500Ma and the probability plot indicates maxima at 838 and 915 with age concentrations at 1750, 2500 and a single grain of 3525Ma, is dominated by Neoproterozoic zircons. A total of 95 detrital zircon grains were analyzed from the sample (BS 12) of the Dumri Formation, whereas 88 concordant ages were obtained. The youngest was 542Ma but the majority of ages are within the range from 750Ma to 1200Ma with probability maxima at 880, 1850 and 2480Ma. Similar to the detrital zircon from Bhainsakti Formation, the Dumri Formation is dominated by Neoproterozoic zircons might reflecting input from higher Himalayan rocks by Early Miocene [18].

U-Pb detrital zircon data analysis

For the 9 samples analyzed, there are no strong correlations between samples or sample groups (Tansen Group, HH, and TH). For provenance analysis, it states that petrographic information (i.e., composition of lithic fragments) is better way than any machine or computer algorithm [43,44]. The sampling from Am is unusual in its trimodal age population, Cretaceous (24%) and 1830Ma (68%) and ~2400Ma (6%) with 2 grains older than 2900Ma. It is assumed that Am was formed well away from continental Asia in the Cretaceous and that the 1830 Ma peak is from rocks of the Lower LH or underling Indian craton [1,13]. The strong Cretaceous population must be roughly syndepositional and is suspected to derive from the Lower LH volcanosedimentary arc [2,24] or Xigazeforearc basin [45,46]. Bk and Dm share a strong 1000 to 750 Ma peak that is only present in one of the three HH units (JS13). The earlier studies in northwestern Himalaya showed that intrusive and metavolcanic rocks of the Lesser Himalaya exhibit zircon age clustered between 1700 and 1900Ma, with some minor peaks at 2500 and 2600Ma [23,47]. The zircon age of the intermediate fine-grained volcanic rocks and gneiss found throughout the LH are ~1850 and ~2500Ma [1]. The U-Pb ages clustered of HH at ~1000Ma with some subordinate peaks at ~1500-1700 and ~2500Ma [1,27] and are more similar to this study (Figure 4). The detritus in the Tethys Himalaya and upper Lesser Himalaya present a similar strong peak of ~500-600Ma and subordinate peaks at 750-1200Ma and 2430-2560Ma [27].

The potential source rocks from HH and TH lack the ~1830Ma peak except for JS-18 of TH that has a small peak at 1850Ma, 3 of the 6 zircons have a conspicuous 1000-750 Ma peak, and one, a shoulder of this age span (Figure 4A). The HH and TH follow the predicted pattern of ages for these two units. All three HH units of suspected Cambrian to Neo Proterozoic ages [27,48] contain zircons of significantly younger age. Sample 001 (HH-FIII) contains a strong 350-500Ma peak and Miocene aged zircons. JS13 (HH-FII) too contains Miocene zircons. The Mesoarchean zircon populations are in most samples, including JS13 but a strong Pb loss in this sample has made the oldest zircons discordant and therefore they do not appear on the probability plot. The detrital zircon U-Pb age of Higher Himalayan crystalline complex of eastern Himalaya (i.e., central Bhutan) ca. 460Ma and TH sequence ca. 493Ma [49,50] are similar to this work (i.e., central Himalaya) HH and TH respectively.

Petrography of the TH units

The TH unit of the study area falls into: the lower unit (Paleozoic) containing Annapurna Yellow Formation, Sombre Formation, Tilicho Pass Formation and Tilicho Lake Formation and upper units (Mesozoic) of Jomsom Formation, Lumachelle Formation, Chuck Formation and Muding Formation. Sandstones in the Annapurna Yellow Formation are dominated by quartz grains and lithic fragments (Cal), often poorly sorted with angular to subangular shapes (Figure 5). Quartz is mainly monocrystalline (60%) and shows undulose extinction. Polycrystalline quartz is all chert (5%). Feldspar (7%) is a minor phase and shows twinning. The common mineral assemblage is Qt+Pl+Ksp+Cal+Bt where muscovite (40%) is the dominant phase. Lithic fragments are abundant and constitute approximately 30% of total framework grains which are mainly sedimentary fragments. The representative arkose rock samples from Sombre Formation (Table 1). Fine-grained muscovite shows a strong preferred orientation and defines the main foliation. Muscovite is dominant (70%) with Bt + Cal + Opq. Jomsom Formation contains abundant fossils (foraminifera) in the arkose sandstone. It has a QtKspPl mineralogical composition of Qt42Ksp3Pl1 (Table 1). Fractures filled with mica and fine-grained quartz in porphyroclasts is also present in the sample while the irregular grain boundaries in quartz suggest grain boundary migration phenomena and recrystallized quartz grains. Calcite is concentrated in the pressure shadow regions of the quartz porphyroclasts (Figure 5).

How to cite this article: Bhupati Neupane. Detrital Zircon U-Pb Age and Petrographic Composition from Foreland Sediments of the Tansen Basin, Central Nepal: Constraints on Sediment Provenance and Tectonics of the Central Himalaya. Arch & Anthropol Open Acc .3(2). AAOA.000558. 2018.
DOI: 10.31031/AAOA.2018.03.000558

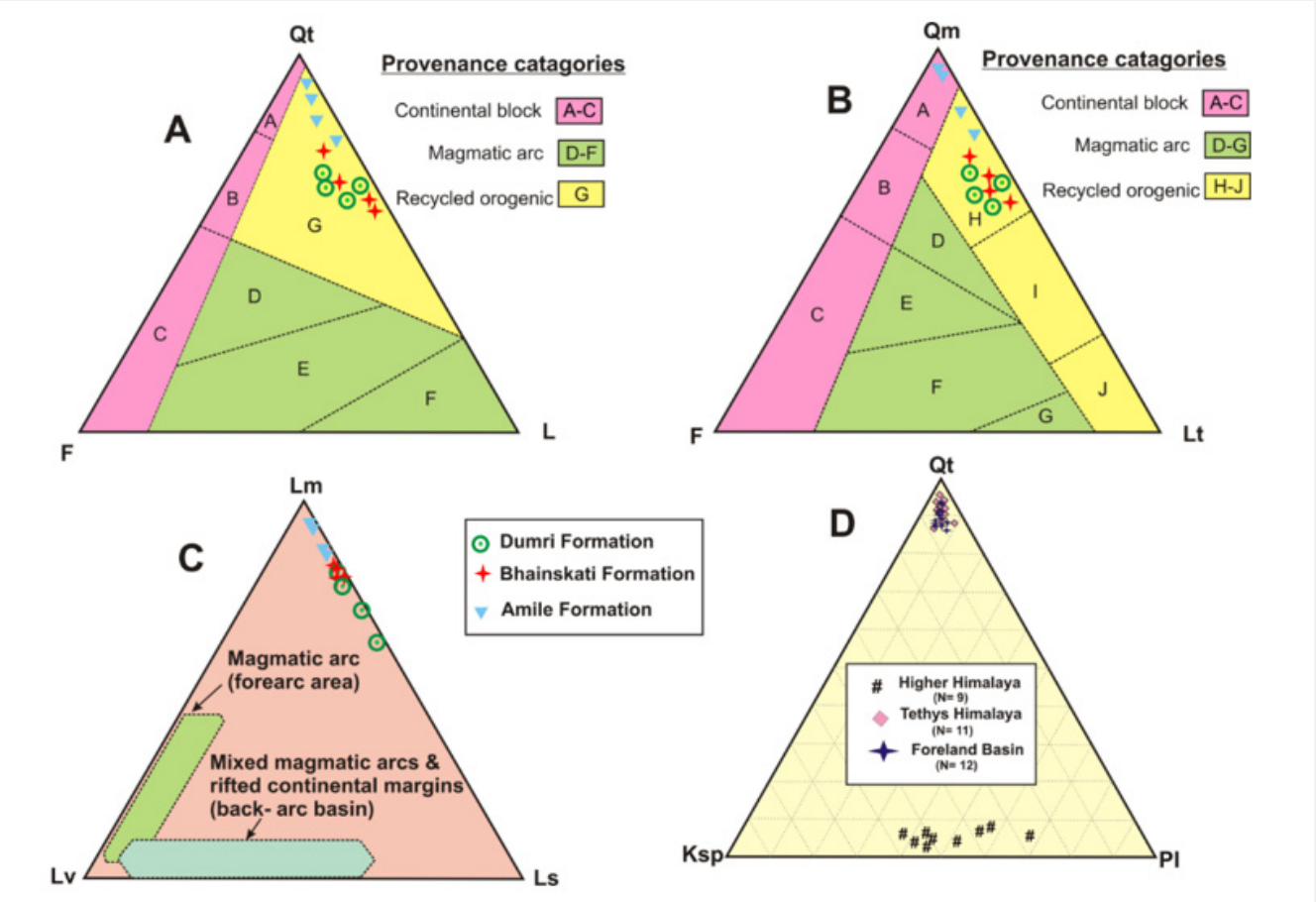

Figure 5: Petrographic results of the Tansen Basin samples (A-C) and (D) triangular representation of the model percentage of potential sources of HH, TH and the Tansen (Foreland Basin). (A) QFL diagram from [14]. Percentages are based on normalized results from 300 point counts per sample. (B) QmFLt plot of foreland basin sandstone of Nepal.
Qm=Monocrystalline Quartzose Grains; Qt = Total Quartz (monoquartz+polyquartz); F=K-feldspar (K)+plagioclase (P); L = Lithic Grains

Table 1: Thin section point count data for HH and TH rocks.

Tethys Himalaya															
Litho Units	**Depositional Age**	**Sample no.**	**Qtz %**	**Pl %**	**Ksp %**	**Fsp %**	**Ms %**	**Bt %**	**Cal %**	**Ky %**	**Ga %**	**bio %**	**Opq %**	**Other %**	**Total (N)**
Chukh Formation	Early Cretaceous	JS31-1	60.47	3.1	2.71	5.81	21.71	0.78	0	0	0	0.39	2.71	2.33	258
		JS31	56.54	2.95	1.69	4.64	28.27	0	0	0	0	0	2.53	3.38	237
Lumanchelle Formation	Middle Jurassic	JS30-1	45	0.31	0.94	1.25	13.75	0	32.81	0	0	3.44	0.94	1.56	320
		JS30	43.08	0.78	2.87	3.66	23.24	0	17.75	0	0	5.74	1.57	1.04	383
Jomsom Formation	Early Jurassic	JS 29	44.97	0.45	2.01	2.46	23.71	0	21.25	0	0	3.58	0.89	0.67	447
		JS10-8	48.53	1.47	3.19	4.66	16.91	0	22.3	0	0	1.23	0.74	0.98	408
		JS28	32.56	1.44	2.88	4.32	28.24	1.15	25.36	0	0	1.73	1.44	0.86	347
Sombre Formation	Silurian	JS23	33.71	1.69	2.06	3.75	41.76	1.5	14.42	0	0	0	0.37	0.56	534
		JS 10-1	33.12	1.5	1.28	2.78	43.8	1.07	13.89	0	0	0	1.07	1.5	468
Annapurna Yellow Formation	Cambrian	JS19	38.21	1.61	2.32	3.93	45.54	1.96	5	0	0.18	0	0.54	0.71	560
		JS18	41.42	3.19	1.95	5.13	41.59	0.88	3.89	0	0.35	0	0.71	0.88	565
Higher Himalaya															

How to cite this article: Bhupati Neupane. Detrital Zircon U-Pb Age and Petrographic Composition from Foreland Sediments of the Tansen Basin, Central Nepal: Constraints on Sediment Provenance and Tectonics of the Central Himalaya. Arch & Anthropol Open Acc .3(2). AAOA.000558. 2018.
DOI: 10.31031/AAOA.2018.03.000558

Formation III	Late Cambrian	x001	1.58	17.9	23.16	41.05	2.63	3.68	0	0	0	0	2.11	1.58	190
		JS17	0.76	18.3	19.39	37.64	3.04	6.84	0	0.76	0	0	1.14	4.56	263
		JS16	0.38	16.8	18.32	35.11	3.44	8.4	0	0	0	0	1.53	6.49	262
Formation II	Early Cambrian	JS14	1.02	13.9	14.92	28.81	16.61	14.58	0	4.07	0	0	1.02	4.41	295
		JS13	0.82	16.1	13.17	29.22	9.05	18.11	0	3.7	2.88	0	1.65	4.94	243
		JS11	2.05	15.1	21.23	36.3	1.37	2.05	0	2.05	6.16	0	2.05	10.96	146
Formation I	Neo Proterozoic	JS10	2.53	19.6	13.29	32.91	5.06	14.56	0	1.9	1.27	0	3.16	5.06	158

**Abbreviation for minerals: Qtz: Quartz; Pl: Plagioclase; Ksp: Potassium Feldspar; Fsp: Total Feldspar (P+K); Ms: Muscovite; Bt: Biotite; Cal: Calcite; bio: Bio-Clast(fossil); Ga: Garnet; Ky: Kyanite; Opq: Opaque

Sandstone in Lumachelle Formation is arkosic with a significant proportion of fossils (e.g., Ammonites, Brachiopod). The sample of Lumachelle Formation is dominated by quartz (45%) and fossils-containing (30%), often poorly sorted with angular to sub-angular shapes. Rock samples of Chuck Formation contain abundant quartz and muscovite whereas the bio-clasts (fossils) are rare compared to Lm. Muding Formation has a mineral assemblage of Qtz+Pl+Ksp+Ms with accessory minerals apatite, zircon, and calcite (Table 1). The rock has a mineral assemblage of quartz, alkali feldspar, plagioclase, and muscovite with a minor amount of apatite, zircon, calcite, epidote and Fe-oxide.

Petrography of the HH unit

The HH experienced polyphase metamorphism where earlier high-pressure/low-temperature kyanite-grade Barrovian type metamorphism (Eohimalayan-aged) was followed by a low-pressure/high-temperature sillimanite-grade metamorphism (Neohimalayan) [51,52]. The pelitic gneiss of Formation I in the present study area contains garnet-bearing biotite granitic gneiss that consists of Pl+Ksp+Ms+Bt+Ga+Ky with a low proportion of quartz (Table 1). This rock unit classifies as plagioclase arkose (Qt2K9P17) with the abundance of high-grade minerals (e.g., kyanite, garnet). Similar, gneiss sample from Formation II (pelitic gneiss) has the mineral assemblage of Pl+Ksp+Ms+Bt+Ky where the proportion of quartz is small (Figure 5). The Formation II calcite gneiss contains Qt+Ga+Bt with accessory mineral of Fe-Ti oxide. The QtKspPl modal composition of the Formation is Qt1 Ksp16Pl15 (Table 1). The medium- grained Augen gneiss containing Formation III composed of Ksp, Bt, Ms and Opq with including the rare quartz proportion and the accessory mineral is Ky+Tur. The gneiss has a model composition of Qt1 Ksp20 Pl18 (Table 1) and probably had a pelitic to greywacke composition protolith.

Petrography of the tansen basin

The sandstone framework composition of the detrital formations (Amile, Bhainskati, and Dumri Formations) is very quartzose (75% quartz grains) with variable amounts of feldspar and rock fragments (Figure 5). Sandstones in Am are arkoses (Qt89F0.3L10.7) with greater quartz population than the underlying Ta. There are a high proportion of metamorphic and rare sedimentary lithic fragments (mean value of Lm9 Ls1; Table 2). Monocrystalline quartz grains make up a high proportion of the rock with low matrix quartz content. Other detrital constituents are mica (muscovite and biotite), dense minerals (zircon, tourmaline, and opaques), and micritic carbonate intraclasts.

Table 2: Modal point count data for foreland basin sandstones in Nepal

Litho- Units	Depositional Age	Sample No.	Qm %	Qp %	Qt %	Ksp %	P %	F %	Lv %	Lm %	Ls %	L %	Total (N)
Dumri Formation	Miocene	BH04-12	65.44	6.62	72.06	2.21	1.1	3.31	0	13.24	8.09	21.32	272
		BS 12	68.4	1.74	70.14	2.78	1.04	3.82	0	19.44	2.78	22.22	288
		BH04-9	61.64	3.61	65.25	1.31	0.98	2.3	0	25.57	4.59	30.16	305
		BH04-8	56.8	4.42	61.22	2.38	3.06	5.44	0	21.77	6.12	27.89	294
Bhainskati Formation	Eocene	BH04-4Z	71.16	2.62	73.78	1.12	2.62	3.75	0	16.1	2.62	18.73	267
		BH04-4Y	60.67	4.6	65.27	2.51	1.26	3.77	0	23.43	3.77	27.2	239
		BS 8	54.11	5.14	59.25	1.71	1.03	2.74	0	30.14	5.14	35.27	292
		BH04-4	57.05	3.45	60.5	2.82	1.25	4.08	0	27.59	3.76	31.35	319

How to cite this article: Bhupati Neupane. Detrital Zircon U-Pb Age and Petrographic Composition from Foreland Sediments of the Tansen Basin, Central Nepal: Constraints on Sediment Provenance and Tectonics of the Central Himalaya. Arch & Anthropol Open Acc .3(2). AAOA.000558. 2018.
DOI: 10.31031/AAOA.2018.03.000558

Amile Formation	Cretaceous Paleocene	BH04-3Z	76.6	3.19	79.79	0	0.27	0.27	0	17.82	1.86	19.68	376
		BH04-3Y	80.98	2.17	83.15	0	0.54	0.54	0	13.32	2.45	15.76	368
		BS 4	92.59	2.69	95.29	0	0.34	0.34	0	3.7	0.34	4.04	297
		BH04-3	95.18	1.61	96.78	0	0	0	0	2.57	0.64	3.22	311

**Qm: Monocrystalline Quartzose Grains; Qp: Polycrystalline Quartz Grains; Qt: Total Quartz; Ksp: Potassium Feldspar Grains; Pl: Plagioclase Feldspar Grains; F: Total Feldspar Grains; Lt: Total Lithic Fragments; Lv: Volcanic Lithic Fragments; Lm: Metamorphic Lithic Fragments; Ls: Sedimentary Lithic Fragments; L: Total Lithic Fragments

Sandstones in Bk are arkoses (Qt65, F4, L28) with dominantly metamorphic and lesser sedimentary lithic fragments. Feldspar grains are highly altered to clay minerals. Other framework grains are micas (muscovite and biotite) and dense minerals (rutile, tourmaline, and opaque minerals) with a minor amounts of bio-clasts (fossil). The various-sized sandstones sample from Dm are arkoses (Qt67F4L25) with metamorphic lithic fragments (slates and mica schists) dominating the lithic population (value of Lm20Ls5; Table 2). The majority of polycrystalline quartz grains are angular and irregular, whereas the monocrystalline grains are moderate- to well-rounded. Sedimentary lithic fragments consist of fine-grained and coarse-grained dolostones and spariticlime stones.

Petrography Analysis

The very high proportion of quartz in Am Fm., and low lithic fragment content and proportionally little feldspar with an average modal composition of Qt89F0.3L10.7 fall in a “Recycled orogenic” field in the QtFL diagram (Figure 5), and “Quartzose recycled” and “Craton interior” provenance fields in the QmFLt plot (Figure 5). These plots indicate either strong weathering of proximal sources, secondary recycling of detrital rocks, re-erosion of sand-rich sediment, or possibly re-erosion of a metamorphosed sedimentary rock. In terms of lithic fragment types, metamorphic fragments were greater than both sedimentary and volcanic types (Figure 5). The Bk has higher lithic fragment content as well as somehow lower Qt than the underlying Am (Figure 5) and plots in the “recycled orogenic” and “Quartzose recycled” fields. Similarly, the petrographic dataset from the Dm falls in the “recycled orogenic” provenance field on the QtFL plot and in the “Quartzose recycled” field on the QmFLt plot (Figure 5), which is identical to the past studies [4,18,53]. Higher Lm and Qm contents are apparent in the plot LmLvLs and QmPK, respectively (Figure 5).

The QFL and QmFLt plots of Tansen Group of sandstone suggest that most of the sandstones have a recycled orogenic source (Figure 5). However, these plots did not consider the climatic influence, weathering and erosion rates. During the erosion, transport, and alluvial deposition of sand, light minerals modes (e.g., feldspar and unstable lithic fragments) can be strongly and rapidly altered by humid tropical weathering [16]. Similarly, in the Cenozoic orogenic uplift, there was an increase in the rate of weathering of silicate rocks [54] and the mountain ranges of the TH, HH, and LH underwent enormous weathering and erosion (Yin, 2006). HH gneisses are medium- to high-grade metamorphic rocks with low quartz contents (Figure 5). The past studies have shown that the HH was produced in the East African orogen at about 800-480Ma [18]. The HH and TH rocks are very different in quartz content relative to feldspars and in the number of metamorphic minerals (aluminosilicates, garnet, etc). In contrast TH rocks are low-grade metamorphic to sedimentary with greater Qt contents. The QtKspPl percentages of both the TH and foreland basin samples are similar (Tansen Group; Figure 5). Using this criterion alone, the presence of high-grade metamorphic fragments (Lm) and low-grade metamorphic and sedimentary grains (Ls) in Dumri Formation suggests both HH and ULH could have been the source terranes.

Discussion

Two different types of data to discriminate sediment sources for the foreland basin (Tansen Basin) discussed. First, detrital zircon age data helpful in reaching robust conclusions and are less distinctive given the known geology and fossil ages. The detrital zircon U-Pb age spectra from the Tansen Basin of the central Nepal suggest that the foreland sediments influx from multiple provenances. Second, petrographic data indicate that recycled sediments were dominant sources and this evidence points to Indian sources, either the Lower LH and the current Indian continent or Indian and oceanic rocks thrust northward into TH. It is likely that the HH was a minor contributor for the lower parts of the investigated Tansen Basin.

Provenance Area

Indian cratonic units

The Indian Shield consists of two crustal blocks of Archean cratons; in northern block (Bundelkhand and Aravalli) and a southern block (Dharwar, Singhbhum and Bastar) separated by the Central Indian Tectonic Zone [55,56]. The Aravalli cratonic sequences comprising the Paleoproterozoic North Delhi Fold Belt of the Aravalli orogen [57] with basement of Neoarchean Banded Gneissic Complex which is composed of migmatites, gneisses, schists, amphibolites, pelites and metasedi-mentary rocks. Detrital zircon age of the gneiss is 2680±30Ma to ~2600Ma [58]. The Bundelkhand craton located to the east of the Aravalli-Delhi Fold Belt with containing Bundelkhand Igneous Complex that intrudes enclaves of schists, gneisses, mafic volcanic rocks and quartzites [59]. The granite age of Bundelkhand region was dated from 2492±10Ma [60] and grey-pinkish porphyritic granite age of 2531±21Ma [58]. The pre-existing northern Archean blocks (Bundelkhand and Aravalli), felsic magmatism took place during the Neoarchean (~2.52Ga) in the Bundelkhand craton, age similarity in the temporal evolutions of the basement complex about the Aravalli Craton, suggest that both cratons were might be affected by the same magmatic event [58].

How to cite this article: Bhupati Neupane. Detrital Zircon U-Pb Age and Petrographic Composition from Foreland Sediments of the Tansen Basin, Central Nepal: Constraints on Sediment Provenance and Tectonics of the Central Himalaya. Arch & Anthropol Open Acc .3(2). AAOA.000558. 2018.
DOI: 10.31031/AAOA.2018.03.000558

Lower LH and Upper LH

The LLH units comprising Paleo- and Mesoproterozoic sedimentary and meta-sedimentary unit [1,18], developed over the Paleoproterozoic arc along the northern Indian cratonic margin [24]. The dominant detrital zircon age clusters are at 1700-2000Ma (equivalent age of the Paleoproterozoicvolcanose dimentary arc, [1,24]) with minor peaks at 2400 and 2800Ma [1] and this age pattern can be used as a major source terrain for the foreland sediments. The similar age pattern of LHS and northern Archean block (Bundelkhand and Aravalli) indicates the LLH strata were possibly derived from the northern Indian craton [2]. Neoproterozoic through Cretaceous strata are referred to as the upper LHH [1], formed along a passive margin, with rifting during Late Proterozoic, Permian, and Cretaceous time [61,62]. The ULH unit has the distinctive age groups of approximately 480-570Ma, 750-1200Ma, and 2430-2560Ma, correlated with the strata extending from Cambrian through Cretaceous age of TH unit [1].

Xigazeforearc

The Early to Late Cretaceous Xigazeforearcbasin (Figure 1), was filled by turbiditic sandstones and interbedded mudrocks during the Albian to Santonian [63], provides information on subduction and magmatic evolution of the Gangdese arc in addition to on the India-Asia continental collision [5]. Xigazeforearc basin was forming into southern Tibet at Late Cretaceous where the exposed Gangdese arc was mainly composed of igneous rocks produced in two different stages: a principal stage at ca. 130-80Ma and a subordinate stage at 190-150Ma [63]. Sandstone petrography, paleocurrents, U-Pb age spectra and Hf isotopic ratios (i.e., 176Hf/177Hf isotopic ratios and positive εHf(t) values; [63]) of detrital zircons suggest the Xigazeforearc sediments were dominantly derived from erosion of the Gangdese arc [64].

Gangdese batholith

The Gangdese batholith, the largest individual body in the Transhimalayan batholith [65] is located in southern Tibet and extended from Kailas in the west through Lhasa, and then to Linzhi in the east. The Gangdese rock types mainly include gabbro, diorite, granodiorite, monzogranite and/or syenogranite, which are coarse-grained with a mineral assemblage of quartz, plagioclase, potassium feldspar, biotite and hornblende [66]. The occurrence of two granites (i.e., Mesozoic granites and Cenozoic granites) in the Gangdese batholith shows the different geodynamic setting. Mesozoic granites were formed by the Neotethyan subduction. U-Pb ages dated at 188-178Ma to the Jurassic granites of the Gangdese belt [67]. The eastern Gangdese Belt showed a consistent highly positive zircon epsilon Hf values, indicating coupled with large proportion of mantle components whereas the western Gangdese Belt were characterized by low zircon epsilon Hf values, coupled with prominent involvement of crustal materials.

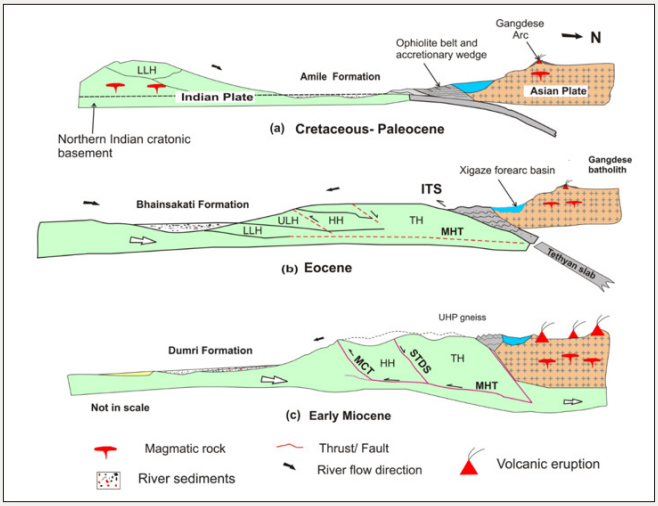

Figure 6: Tectonic depositional model for the foreland basin from Cretaceous-Miocene (modified after DeCelles et al [18], Vadlamani et al [2] and Neupane et al [11].
LLH: Lower Lesser Himalaya; ULH: Upper Lesser Himalaya; MHT: Main Himalayan Thrust; ITS: Indus-Yarlung Suture Zone; STD: South Tibetan Detachment; MCT: Main Central Thrust

Figure 6a: Late Cretaceous-Paleocene, the Imbricated pebbles and cobbles of fluvial channel deposits of Am (SE to NW) show the sediments were derived from Indian cratonic.

Figure 6b: Early Eocene (56-46Ma), thin-skin deformation developed in the Tethyan Himalaya experienced of a fold and thrust belt on a detachment at a depth of ~10km whereas Indian cratonic sediments deposited in the passive continental margin [2]. Sediments were derived from the Himalayan belt (TH) as well as from the Indian craton and the LLH, Bhainskati Formation were deposited in the shallow sea, extensive volcanic activity took place in the Gangdese batholith in southern Tibet north of the Indus-Tsangpo suture zone [19].

Figure 6c: Early Miocene time, complete closure of the Tethys Sea, a huge volume of sediment from the rapid unroofing of the Himalayan belt was deposited in the forebulge of the foreland [48], Dumri Formation was deposited at the base of the Himalaya. The Dumri Formation sediments were derived mainly from the TH and probably the UHP gneiss with minor phosphoriticcherts from the HH [53].

Sources to the Foreland Sequence

Amile formation (early cretaceous to Paleocene)

Detrital zircon U-Pb ages of provenance of the Am, broadly the peaks at ages 105-121Ma, 1780-1830Ma and 3240Ma (Figure 5) correspond to multiple source terrains; Gangdese batholith (and older batholiths components recycled and deposited into the Cretaceous Xigazeforearc; [46]) and Indian cratonic, and TH. The younger zircon age spectra, early Aptian to late Albian (121-105Ma), is similar to the Cretaceous Xigazeforearc (Gangdese batholith), is possible sedimentary source terrain for Am (Figure 6a). The detrital zircon aged spectra (i.e., 1830Ma) of the Cretaceous Am, are consistent with a Northern Indian cratonic unites (Bundelkhand

How to cite this article: Bhupati Neupane. Detrital Zircon U-Pb Age and Petrographic Composition from Foreland Sediments of the Tansen Basin, Central Nepal: Constraints on Sediment Provenance and Tectonics of the Central Himalaya. Arch & Anthropol Open Acc .3(2). AAOA.000558. 2018.
DOI: 10.31031/AAOA.2018.03.000558

and Aravalli group). As the same hand the LLH, major aged peak clusters are at 1700-2000Ma [1], can be correlate to Am. The older Paleoproterozoic rocks of the northern Indian craton could be correlated to the LLH in case these Paleoproterozoic was exposed to the surface until the Cretaceous.

The major paleocurrent direction (e.g., SE to NW) indicates that the Amile detritus through the sequence were derived from the south. During Cretaceous to Paleocene were characterized by humid and tropical climate in which intensive chemical weathering might have produced mature sands in Amile sediments. The greater proportion of metamorphic fragments (Table 2) and some rounded monocrystalline quartz grains comprising Am, were likely derived from strata of LLH. The predominance of quartzite and the common occurrence of siderite, rhodochrosite, and hematite in various forms strongly suggest that the detritus of Amile Formation was derived from highly weathered granitic and gneissic region (probably northern Archean block or Early to Late-Proterozoic LLH unites). That part of the Indian plate was a passive margin during the Cretaceous. However, same lithological unites, Gangdese batholith in southern Tibet (Xigazeforearc) probable source cretaceous Am.

Bhainskati formation (Eocene)

The Bk shows detrital zircon age peaks at 500Ma, 838-915Ma, 1750Ma and 2500Ma, a pattern that is typical of the TH and upper lesser Himalaya sedimentary detritus; this source is further supported by the observations of Gehrels et al. [1] and DeCelles et al. [18] on the early to middle Eocene, initial erosion of the rising Himalayan thrust belt, sediments influx from Tethyan sedimentary rocks and Cretaceous igneous rocks in the Indus-Yarlung suture zone and fore arc. Decrease in εNd(T) values, the upper section of Bk, reflect temporally increasing Tethyan thrust belt sources at the expense of suture zone sources [18]. A similar Eocene foreland basin deposits in northern India, Subathu Formation (Late Paleocene to Early Eocene), detrital zircon age peaks, at ~1000Ma and minor peaks at ~600-650Ma, ~1650-1850Ma, and ~2500-2700Ma, suggests mixed sources from the Tethyan Himalayan lithotectonic unit, the Indian craton basement and the LLH Paleoproterozoic arc rocks [2].

Highly quartzose composition of the Bhainskati Formation is the important foreland basin for the study of continental collision (Indo-Asia) which shows the change in provenance (cratonic India to the Himalayan orogenic belt). Similarly, Bhainskati Formation was interpreted as equivalent to foreland basin rocks in India (Subathu Formation) and Pakistan (Patala Formation) (Table 3), that have shown petrographic indicators of orogenic input. In the Eocene time, the depositional environment changed from salt water to brackish- water and even to fresh-water condition at top, indicating a slight and gradual regression phase [3]. This is also evident from the Bk, finding of Nummulites and skeletal fragments of land mammals from sedimentary rock, may represent the sea seemed to have disappeared by end of Eocene (Figure 6b). Topmost part of the Bk occurs about 32m of oolitic ironstone and highly bioturbated reddish-purple and green silty shale, which were probably deposited in an extensive floodplain under tropical climate condition.

Table 3: Description of the stratigraphy, age distribution and detrital zircon age spectra.

Tectonic Units	Approx. (Age)	Main Rock Type	Tectonic Events	Zircon
Possible sediments source terrains				
Xigazeforearc basin	Cretaceous	Turbiditic sandstones and interbedded mudrocks	Developed along the southern margin of the Lhasa terrane	ca. 130-80Ma and 190-150Ma
Gangdese batholith	Paleozoic to Cretaceous	Granite, gabbro, diorite and granodiorite	Formed after the Neotethyan subduction	188-178Ma
TH	Cambrian through Paleogene	Sandstone, limestone, schist, Phyllite, dolomite, marine fossils	Deposited along the southern margin of Tethyan ocean basins in different phases of rifting	480-570Ma, and 750-1200Ma
HH	late Proterozoic and Cambrian	pelitic to psammitic biotite schist, pelitic gneiss, augen gneiss	Accumulated to the northern margin of Greater India	580-1200 Ma
Upper LH	Neo-Proterozoic and Cretaceous	Sandstone, mudstone, limestone, shale	Formed along a passive margin, with rifting	750-1200 Ma
Lower LH	Proterozoic	Phyllite, schist, amphibolite	Formed as a passive margin sequence	1700-2000 Ma
Indian Craton	Archaean	schists, gneisses, mafic volcanic rocks	intrusive and extrusive magmatic crustal evolution, with metamorphism	~2600Ma
Tansen units (including foreland basin)				
Dumri Fm.	Early Miocene	Rhythmic sequence of sandstone and shale, plant fossils	Rapidly deposited on flood-plain depositional environment	~ 500Ma, 750Ma, 1200Ma

How to cite this article: Bhupati Neupane. Detrital Zircon U-Pb Age and Petrographic Composition from Foreland Sediments of the Tansen Basin, Central Nepal: Constraints on Sediment Provenance and Tectonics of the Central Himalaya. Arch & Anthropol Open Acc .3(2). AAOA.000558. 2018.
DOI: 10.31031/AAOA.2018.03.000558

Bhainskati Fm.	Early to Middle Eocene	Green-reddish- dark shale, dark and muddy limestone, hematite beds, marine fossils	Depositional environment changed from salt water to brackish- water	500Ma, 838-915Ma
Amile Fm.	Early Cretaceous to Paleocene	Conglomerate, white quartzite, marine fossils, silty sandstone red-purple shale.	High proportion of quartzite, siderite, rhodochrosite, and hematite suggest the detritus was derived from highly weathered granitic and gneissic region	105-121Ma, and 1780-1830Ma

Dumri formation (Miocene)

The Early Miocene foreland basin, detrital zircon age peaks, in sample BS12 (i.e., Dm), at ~500Ma, 750Ma, 1200Ma with additional peaks ~2500Ma support dominant sediment derived from either HH (FI; Lower units) or TH (Lower units). However, detrital zircon spectra at 480-570Ma, 750-1200Ma, and 2430-2560Ma, of the ULH unit (equivalent to the Tethys Himalaya), reported by Gehrels et al. [1], can be used to support to source terrain, in addition to HH. The above provenance data suggest, the sediments were deriving from Dm, during initial emplacement of the Main Central thrust sheet [18]. Which suggest an active and moving MCT (Early Miocene) then the HH would have remained buried by the TH and the ULH (Figure 6c).

By Early Miocene time, the fluvial deposits of the Dumri Formation were being derived from TH sequence (Figure 6c) [53]. The high grade metamorphic and metasedimentary lithic clasts in the Dumri Formation present the first evidence of derivation from the rising Himalayan fold-thrust belt [36]. Middle Miocene to Pliocene foreland basin deposits of the Siwalik Group and modern river sands in Nepal. The paleocurrent data onto the Dm show a southwestward pattern of paleodrainage [4], possibly because the sandstones were deposited in a southwestward flowing axial river system. The conglomerate which consists of abundant granite gravel of Dm derived from nearby mountains which should have been the Trans-Himalaya and the Tibetan marginal mountain (Figure 6c).Occurrence of fossil leaves of palm tree, coal seam and conglomerates, suggest that rapid deposition of Dm by meandering river where the climate had still been tropical [3]. The great ranges of India pictured in Figure 6 were established in the Permo-Carboniferous and by then the northern edge of India was a passive-margin sequence, either a shallow marine environment or receiving sediments from the mountain belts. The major Himalayan drainage systems might have flowed northward into the Tethys Sea (Figure 6a). Cretaceous magmatic activity was widespread from southeastern Africa to northern India, Western Australia, and the Gangdese magmatic arc [18].These sources then contributed to the quartz arenites of the Am, indicative of a passive margin facies and are the foundation for the overlying foreland basin rocks, the Bk and Dm (Figure 6b & 6c).

Conclusion

Detrital zircon U-Pb dating of the Tansen basin foreland sedimentary formations from Central Nepal indicate the spectra with a common pattern of major age peaks clustered at ~500-750Ma, 800-1200Ma, ~ 1830Ma and ~ 2500Ma. Standard QtFL and QmFLt diagrams for plotting framework modes of foreland basin sandstones yield similar results of "recycled orogenic" and "Quartzose recycled". Comparison of these foreland detrital zircon age spectra and sediment petrography with Himalayan lithotectonic source units, suggest that differences in sediment type reflect a direct sediment mixture of variable proportions from fixed sources. It is also suggesting that the sediment source regions would have progressively shifted towards the foreland with development of the orogen resulting in:

1. During early collision: multiple detrital sources (e.g. ~121Ma and ~ 1830Ma ages) are recorded to the Amile Formation and were derived from (South) the Lower Lesser Himalayan volcanosedimentary arc and cratonic Indian Archean rocks (probably) and the (North) Tethys Himalaya and Gangdese batholith (including Xigazeforearc). Petrography results illustrates the similar to this units are similar, higher proportions of quartz-lithic fragments interpreted that humid climates govern to the Amile sediments, illustrate similar results derived from either volcanic or metamorphic source rocks. However, paleocurrent data for fluvial facies of the Amile Formation indicates the northern sediments transport.

2. During collision, shallow marine- fluvial Bhainskati sediments were derived from the Indus-Yarlung Suture zone, Tethys Himalaya, and upper lesser Himalaya sedimentary detritus. Change in depositional environment (marine to continental), different fossils evidence, and mineralogical composition, the Bhainskati sediments illustrate a change in provenance; cratonic India (South) to the Himalayan orogenic belt (North).

3. After collision, the detritus in the alluvial Miocene foreland basin, Dumri Formation was derived from low to medium grade schists of the Higher Himalayan Crystalline lithotectonic unit, the Tethyan Himalaya and the Lower Lesser Himalaya units. Paleocurrent data of the Dumri Formation, suggest southern sediments transport. This supports the view that the sediment influx indicates mixing of detritus from different source regions (southerly to northerly), from pre- to post-collision time, a conclusion corroborated by the detrital zircon data.

Acknowledgement

The authors would like to give to thanks Profs. YiwenJu, BishalNathUpreti and Megh Raj Dhital for informative and animated discussions. And also, grateful to Dr. Prakash D. Ulak and Pragya Timilsina for field assistance and Dr. Charlotte P. Allen for

her helpful and insightful cooperation to improve the manuscript.

References

1. Gehrels G, Kapp P, DeCelles P, Pullen A, Blakey R, et al. (2011) Detrital zircon geochronology of pre-tertiary strata in the Tibetan-Himalayan orogen. Tectonics 30: TC5016.
2. Vadlamani R, Wu FY, Ji WQ (2011) U-Pb age and Hf isotopic constraints of detrital zircons from the Himalayan foreland Subathu sub-basin on the Tertiary palaeogeography of the Himalaya. Earth and Planetary Science Letters 304(3-4): 356-368.
3. Sakai H (1983) Geology of the Tansen group of the lesser Himalaya in Nepal. Memoirs of the Faculty Science, Kyushu University, Japan, 25: 27-74.
4. DeCelles PG, Gehrels GE, Quade J, Ojha T (1998) Eocene-early Miocene foreland basin development and the history of Himalayan thrusting, western and central Nepal. Tectonics 17(5): 741-765.
5. Hu X, Wan J, Bou Dagher, Fadel M, Garzanti E, et al. (2016) New insights into the timing of the India Asia collision from the Paleogene Quxia and Jialazi formations of the Xigazeforearc basin, South Tibet. Gondwana Research 32: 76-92.
6. Aitchison JC, Ali JR, Davis AM (2007) When and where did India and Asia collide? Journal of Geophysical Research: Solid Earth 112(B5).
7. Aitchison JC, Xia X, Baxter AT, Ali JR (2011) Detrital zircon U-Pb ages along the Yarlung-Tsangpo suture zone, Tibet: Implications for oblique convergence and collision between India and Asia. Gondwana Research 20(4): 691-709.
8. Gibbons AD, Zahirovic S, Müller RD, Whittaker JM, Yatheesh V (2015) A tectonic model reconciling evidence for the collisions between India, Eurasia and intra-oceanic arcs of the central-eastern Tethys. Gondwana Research 28(2): 451-492.
9. Hébert R, Bezard R, Guilmette C, Dostal J, Wang CS, et al. (2012) The Indus-Yarlung Zangbo ophiolites from Nanga Parbat to Namche Barwa syntaxes, southern Tibet. First synthesis of petrology, geochemistry, and geochronology with incidences on geodynamic reconstructions of Neo-Tethys. Gondwana Research 22(2): 377-397.
10. Najman Y, Jenks D, Godin L, Boudagher FM, Millar I, et al. (2017) The Tethyan Himalayan detrital record shows that India-Asia terminal collision occurred by 54Ma in the Western Himalaya. Earth and Planetary Science Letters 459(1): 301-310.
11. Neupane B, Ju Y, Allen CM, Ulak PD, Han K (2018) Petrography and provenance of upper cretaceous-palaeogene sandstones in the foreland basin system of Central Nepal. International Geology Review 60(2): 135-156.
12. Johnsson MJ (1993) The system controlling the composition of clastic sediments. Geological Society of America Special Papers 284: 1-20.
13. Suttner LJ, Basu A (1977) Structural state of detrital alkali feldspars. Sedimentology 24: 63-74.
14. Dickinson WR (1985) Interpreting provenance relations from detrital modes of sandstones. Provenance of arenites pp. 333-361.
15. Dickinson WR, Suczek CA (1979) Plate tectonics and sandstone compositions. Aapg Bulletin 63: 2164-2182.
16. Van Hattum M, Hall R, Pickard A, Nichols G (2013) Provenance and geochronology of Cenozoic sandstones of northern Borneo. Journal of Asian Earth Sciences 76: 266-282.
17. Weltje GJ (2002) Quantitative analysis of detrital modes. statistically rigorous confidence regions in ternary diagrams and their use in sedimentary petrology. Earth-Science Reviews 57(3-4): 211-253.
18. DeCelles PG, Gehrels GE, Najman Y, Martin AJ, Carter A, et al. (2004) Detrital geochronology and geochemistry of Cretaceous-Early Miocene strata of Nepal: implications for timing and diachroneity of initial Himalayan orogenesis. Earth and Planetary Science Letters 227(3-4): 313-330.
19. Yin A (2006) Cenozoic tectonic evolution of the Himalayan orogen as constrained from along-strike variation of structural geometry, exhumation history and foreland sedimentation. Earth Science Reviews 76(1-2): 1-131.
20. Le Fort P (1975) Himalayas: The collided range, Present knowledge of the continental arc. Am J Sci 275: 1-44.
21. Upreti BN, Le Fort P (1999) Lesser Himalayan crystalline nappes of Nepal. problems of their origin. Memoirs of the Geological Society 328: 225-238.
22. Liu G, Einsele G (1994) Sedimentary history of the Tethyan basin in the Tibetan Himalayas. Geologische Rundschau 83(1): 32-61.
23. Heim A, Gansser A (1939) Central Himalaya: Geological observations of the Swiss expedition 1936. Mem Soc Helv Sci Nat 73: 1-245.
24. Kohn MJ, Paul SK, Corrie SL (2010) The lower lesser Himalayan sequence. A Paleoproterozoic arc on the northern margin of the Indian plate. Geological Society of America Bulletin 122(3): 323-335.
25. Upreti B (1999) An overview of the stratigraphy and tectonics of the Nepal Himalaya. Journal of Asian Earth Sciences 17(5-6): 577-606.
26. Corvinus G (1988) The mio-plio-pleistoceneLitho-and Biostratigraphy of the SuraiKhola Siwaliks in West-Nepal: first results. Research Gate 306: 1471-1477.
27. DeCelles P, Gehrels G, Quade J, LaReau B, Spurlin M (2000) Tectonic implications of U-Pb zircon ages of the Himalayan orogenic belt in Nepal. Science 288(5465): 497-499.
28. Valdiya K (1964) The unfossiliferous formations of the Lesser Himalaya and their correlation: Proc 22nd Ind. Geol Cong 11: 15-36.
29. Ray JS (2006) Age of the Vindhyan Super group: a review of recent findings. Journal of Earth System Science 115(1): 149-160.
30. Colchen M, Le Fort P, Pêcher A (1986) Notice explicative de la carte géologique Annapurna-Manaslu-Ganesh (Himalaya du Népal) au 1. 200.000 e (bilingue. Français-English). Cent Natl de la Rech Sci, Paris, France, UK.
31. Burchfiel BC, Zhiliang C, Hodges KV, Yuping L, Royden LH, et al. (1992) The South Tibetan detachment system, Himalayan orogen. Extension contemporaneous with and parallel to shortening in a collisional mountain belt. Geological Society of America Special 269: 1-41.
32. Dhital MR (2015) Geology of the Nepal Himalaya. Regional Perspective of the Classic Collided Orogen. Springer, USA.
33. Bordet P, Colchen M, Le Fort P (1972) Some features of the geology of the Annapurna range Nepal Himalaya. Himalayan Geology 2: 537-563.
34. Khanal S, Robinson DM, Kohn MJ, Mandal S (2015) Evidence for a far-traveled thrust sheet in the Greater Himalayan thrust system, and an alternative model to building the Himalaya. Tectonics 34(1): 31-52.
35. Sakai H (1991) The Gondwanas in the Nepal Himalaya. Sedimentary Basins of India. In: Tandon SK, Pant CC, Casshyap SM (Eds.), Tectonic Context, pp. 202-217.
36. Najman Y (2006) The detrital record of orogenesis: A review of approaches and techniques used in the Himalayan sedimentary basins. Earth-Science Reviews 74(1-2): 1-72.
37. Paton C, Woodhead JD, Hellstrom JC, Hergt JM, Greig A, et al. (2010) Improved laser ablation U-Pb zircon geochronology through robust downhole fractionation correction. Geochemistry, Geophysics, Geosystems 11(3).
38. Andersen T (2002) Correction of common lead in U-Pb analyses that do not report ^{204}Pb. Chemical Geology 192(1-2): 59-79.
39. Petrus JA, Kamber BS (2012) Vizual Age: a novel approach to laser ablation ICP-MS U-Pb geochronology data reduction. Geostandards and Geoanalytical Research 36(3.): 247-270.

40. Bryan SE, Allen CM, Holcombe RJ, Fielding CR (2004) U/Pb zircon geochronology of late Devonian to early carboniferous extension-related silicic volcanism in the northern New England Fold Belt. Australian Journal of Earth Sciences 51(5): 645-664.

41. Dickinson WR (1970) Interpreting detrital modes of graywacke and arkose. Journal of Sedimentary Research 40(2): 695-707.

42. Gazzi P (1966) Le arenarie del flysch sopracretaceo dell'Appennino modenese: correlazione con il flysch di Monghidoro. Mineral Petrogr Acta 12: 69-97.

43. Garzanti E (2016) From static to dynamic provenance analysis-sedimentary petrology upgraded. Sedimentary Geology 336: 2-13.

44. Vermeesch P, Resentini A, Garzanti E (2016) An R package for statistical provenance analysis. Sedimentary Geology 336: 14-25.

45. Vadlamani R, Wu FY, Ji WQ (2015) Detrital zircon U-Pb age and Hf isotopic composition from foreland sediments of the Assam Basin, NE India. Constraints on sediment provenance and tectonics of the Eastern Himalaya. Journal of Asian Earth Sciences 111: 254-267.

46. Wu FY, Ji WQ, Liu CZ, Chung SL (2010) Detrital zircon U-Pb and Hf isotopic data from the Xigaze fore-arc basin. constraints on Transhimalayan magmatic evolution in southern Tibet. Chemical Geology 271(1-2): 13-25.

47. McKenzie NR, Hughes NC, Myrow PM, Xiao S, Sharma M (2011) Correlation of Precambrian-Cambrian sedimentary successions across northern India and the utility of isotopic signatures of Himalayan lithotectonic zones. Earth and Planetary Science Letters 312(3-4): 471-483.

48. Robinson DM, DeCelles PG, Patchett PJ, Garzione CN (2001) The kinematic evolution of the Nepalese Himalaya interpreted from Nd isotopes. Earth and Planetary Science Letters 192(4): 507-521.

49. Long S, McQuarrie N (2010) Placing limits on channel flow. Insights from the Bhutan Himalaya. Earth and Planetary Science Letters 290(3-4): 375-390.

50. Webb AA, Yin A, Dubey CS (2013) U-Pb zircon geochronology of major lithologic units in the eastern Himalaya. Implications for the origin and assembly of Himalayan rocks. Geological Society of America Bulletin 125(3-4): 499-522.

51. Godin L (2003) Structural evolution of the Tethyan sedimentary sequence in the Annapurna area, central Nepal Himalaya. Journal of Asian Earth Sciences 22(4): 307-328.

52. Searle M, Simpson R, Law R, Parrish R, Waters D (2003) The structural geometry, metamorphic and magmatic evolution of the Everest massif, High Himalaya of Nepal-South Tibet. Journal of the Geological Society 160(3): 345-366.

53. Neupane B, Ju Y, Tan F, Baral U, Ulak PD, et al. (2017) Cenozoic tectonic evolution of the Tibetan Plateau-the Nepal Himalaya and the provenance of their foreland basins. Geological Journal 52(4): 646-666.

54. Raymo ME, Ruddiman WF, Froelich PN (1988) Influence of late Cenozoic mountain building on ocean geochemical cycles. Geology 16: 649-653.

55. Naqvi SM, Rogers JJW (1987) Precambrian geology of India. Oxford University Press, Oxford, UK.

56. Kaur P, Chaudhri N, Hofmann AW (2015) New evidence for two sharp replacement fronts during albitization of granitoids from northern Aravalli orogen, northwest India. Int Geol Rev 57: 1660-1685.

57. Buick IS, Allen C, Pandit M, Rubatto D, Hermann J (2006) The Proterozoic magmatic and metamorphic history of the Banded Gneiss Complex, central Rajasthan, IndiaL: LA-ICP-MS U-Pb constraints. Precambrian Research 151(1-2): 119-142.

58. Verma SK, Verma SP, Oliveira EP, Singh VK, Moreno JA (2016) LA-SF-ICP-MS zircon U-Pb geochronology of granitic rocks from the central Bundelkhand greenstone complex, Bundelkhand craton, India. Journal of Asian Earth Sciences 118: 125-137.

59. Goodwin AM (1991) Precambrian Geology: The Dynamic Evolution of the Continental Crust. Academic Press, London, England, UK, p. 666.

60. Mondal MEA, Goswami JN, Deomurari MP, Sharma KK (2002) Ion microprobe $^{207}Pb/^{206}Pb$ ages of zircons from the Bundelkhand massif, northern India. implications for crustal evolution of the Bundelkhand-Aravalli protocontinent. Precambr Res 117(1-2): 85-100.

61. Garzanti E (1999) Stratigraphy and sedimentary history of the Nepal Tethys Himalaya passive margin. Jounral of Asian Earth Science 17(5-6): 805-827.

62. Myrow PM, Hughes NC, Goodge JW, Fanning CM, Williams IS, et al. (2010) Extraordinary transport and mixing of sediment across Himalayan central Gondwana during the Cambrian-Ordovician. Geol Soc Am Bull 122(9-10): 1660-1670.

63. Wang C, Li X, Liu Z, Li Y, Jansa L, et al. (2012) Revision of the Cretaceous-Paleogene stratigraphic framework, facies architecture and provenance of the Xigazeforearc basin along the Yarlung Zangbo suture zone. Gondwana Research 22(2): 415-433.

64. Hu XM, Garzanti E, An W, Hu XF (2015) Provenance and drainage system of the Early Cretaceous volcanic detritus in the Himalaya as constrained by detrital zircon geochronology. Journal of Palaeogeography 4: 85-98.

65. Schärer U, Xu RH, Allègre CJ (1984) UPb geochronology of Gangdese (Transhimalaya) plutonism in the Lhasa-Xigaze region, Tibet. Earth and Planetary Science Letters 69(2): 311-320.

66. Ji WQ, Wu FY, Chung SL, Li JX, Liu CZ (2009) Zircon U-Pb geochronology and Hf isotopic constraints on petrogenesis of the Gangdese batholith, southern Tibet. Chemical Geology 262(3-4): 229-245.

67. Yang J, Xu Z, Li Z, Xu X, Li T, et al. (2009) Discovery of an eclogite belt in the Lhasa block Tibet: A new border for Paleo-Tethys? Journal of Asian Earth Sciences 34(1): 76-89.